

Diffusion Curvature for Fast, Point-wise, Noise-Resistant Geometric Featurization of Graphs and Pointclouds

Kincaid MacDonald Dhananjay Bhaskar Kaly Zhang
Ian Adelstein Smita Krishnaswamy

2024-05-09

For a number of years now work has been proceeding in order to bring to perfection the crudely conceived idea of a machine that would not only supply inverse reactive current for use in unilateral phase detractors, but would also be capable of automatically synchronizing cardinal grammeters. Such a machine is the “Turbo-Encabulator.”

0.1 Introduction

One of the most ubiquitous subjects of analysis in data science is the humble point cloud. The points, by themselves, are high dimensional and noisy; it is up to the data scientist to wring sense out of them. Per the Manifold Hypothesis, we assume the points were sampled on or near the surface of a low-dimensional manifold embedded in high-dimensional Euclidean space. Manifold learning methods, like t-SNE, PHATE, and Diffusion Maps [(maaten2008VisualizingDataUsing?)](moon2019VisualizingStructureTransitions?)(coifman2006D endeavor to recover salient features of the underlying manifold, like geodesic distances, population clusterings, and dimension, from its high-dimensional noisy sampling.

Curvature is a particularly troublesome geometric property to translate into the discrete, sampled realm. In smooth Riemannian manifolds, curvature is a *local* phenomenon. It can be obtained by fitting osculating circles of radius limiting to zero, or computed from the manifold’s Hessian, using the Second Fundamental Form. None of these translate into the discrete realm. In a sampled manifold, taking a local limit is impossible – one can’t “zoom in” past the sampling of points – and we don’t have access to the parametrization of the manifold or its tangent bundle, without computationally costly and potentially error-prone estimation. Moreover, as our sampling is likely noisy, the curvature can only be recovered over a sufficiently

large neighborhood of points to counter the spurious geometric artifacts created noisy sampling. Thus, in the discrete realm, curvature becomes a “semi-local” phenomenon, in which neither the smallest nor larger scales can be trusted.

There are elegant generalizations of classical curvature to discrete spaces that overcome many of these roadblocks. Ollivier’s *Coarse Ricci Curvature* (CRC) employs optimal transport theory to relate the behavior of a discrete neighborhood to its smooth counterpart (ollivier2009RicciCurvatureMarkov?). Sturm’s *displacement convexity of entropy* (DCE) measures the proliferation of midpoints in positive curvature (sturm2006GeometryMetricMeasure?). Both methods use optimal transport as the basis of their “semi-local” measurement. Rather than trying to zoom in on a point, they define curvature between pairs of points, approximating, at a coarse scale, a Ricci tangent vector.

Although these techniques are theoretically elegant, general, and applicable to any metric measure space, the setting of noisily sampled point clouds is practically challenging for CRC and DCE. Both methods rely on the graph’s shortest-path lengths as an approximation of the manifold’s ground distance - a perilous assumption when dealing with noisy data. And for large datasets, optimal transport calculations can be computationally prohibitive.

In this paper, we develop Diffusion Curvature, a fast curvature estimate derived solely from the graph diffusion matrix. We first introduced the ideas behind Diffusion Curvature in (Bhaskar et al. 2022), in which we demonstrated its ability to produce an unsigned magnitude of curvature estimation for toy datasets and single-cell data, and proved a correspondence between the ratios of scalar curvature and diffusion curvature. We now present a refined definition which produces *signed* curvature values and prove bounds relating Diffusion Curvature to Ollivier’s coarse Ricci Curvature. We demonstrate Diffusion Curvature’s robustness to noise and sampling artifacts, and position our technique as an adaptation of coarse Ricci curvature particularly suitable for point cloud data.

0.2 Background

0.2.1 Curvature in the Continuous Setting

0.2.2 The Discrete Setting

Within the ambient setting of points $x_i \in \mathbb{R}^D$, the Euclidean distances between the points in our point cloud are not very useful. To perform geometric analysis, we want the manifold’s *geodesic* distances between $x_i, x_{j \in \mathcal{M}}$. However, manifolds are locally euclidean, so within a sufficiently small neighborhood of $x_i \in \mathcal{M}$, the euclidean distances are accurate. This is the basis of graph construction: retain only the trustworthy local distances, discard the rest, and then “integrate” over the local neighborhoods to recover features of the global geometry.

A graph $G = (V, E)$ is a collection of n vertices $v_i \in V$ connected by (possibly weighted) edges $e_{ij} \in E$. It is efficiently represented by a single *adjacency* (or *affinity*) matrix $A \in \mathbb{R}^{n \times n}$, where A_{ij} expresses the degree of connection between the vertices v_i and v_j . In a binary adjacency matrix, $A_{ij} = 1$ iff there is an edge between v_i and v_j . In a weighted affinity matrix, $0 < A_{ij} < 1$ with a higher affinity indicating a closer connection between the nodes.

One can construct an affinity matrix from a point cloud with the following algorithm: 1. Compute the matrix D of pairwise euclidean distances between points, so that $D_{ij} = \|x_i - x_j\|_2$. 2. Apply a kernel κ to the distances to construct the affinity matrix, where $A_{ij} = \kappa(D_{ij})$. This is typically the gaussian kernel:

$$k(y) = \frac{1}{\sqrt{2\pi}\sigma} \exp\left(-\frac{y^2}{2\sigma^2}\right)$$

There are a variety of heuristics for selecting an appropriate kernel bandwidth σ . In this paper, we use an adaptive kernel bandwidth, in which, when computing $k(D_{ij})$, σ is set to the mean distance from the points x_i and x_j to their k -th nearest neighbor.

After building our graph affinity matrix A , we created a new representation of the point cloud X – turning it from an $n \times D$ matrix of unwieldy ambient coordinates into an $n \times n$ matrix of pairwise connections between points. The challenge is now to reassemble this information of local connectivity to recover the features of \mathcal{M} . Graph diffusion does precisely this.

0.2.3 Graph Diffusion

The graph diffusion matrix P is a commonly-used method of “integrating” the local connectivity of the graph A into global geometric descriptors of \mathcal{M} . Coifman and Lafon (WAWA YEAR) proved a correspondence between iterated graph diffusion P^t and the Neumann heat kernel on \mathcal{M} . Their technique, *Diffusion Maps*, uses the euclidean distances between eigencoordinates of P to approximate the geodesic distances on \mathcal{M} . The visualization technique *PHATE* (moon2019VisualizingStructureTransitions?) constructs a low-dimensional embedding of a point cloud X such that a distance between the transition probabilities P of X is preserved in the embedding. (More on properties of phate, trajectory preservation.) *Diffusion Earth Mover’s Distance* (tongDiffusionEarthMover2021?) efficiently approximates the transportation distance between distributions on a graph using multi-scale wavelet transform obtained by applying different scales of diffusion. *LEGSNet*’s “learnable geometric scattering” computes tunable scales of diffusion with a graph neural network and achieves state of the art performance on biochemistry graph classification (tong2020DataDrivenLearningGeometric?). These are but a few of the many manifold learning techniques based in diffusion.

Constructing the diffusion matrix from the affinity matrix A is straightforward: you simply row-normalize A , with an optional step to normalizing by density.

Here is the algorithm presented in Coifman and Lafon (coifman2006DiffusionMaps?):

1. (Optional) Compute an *anisotropic density normalization* on A , obtaining the anisotropic adjacency matrix A_\star .
2. Construct the degree matrix D , whose diagonal entries are the rowsums of A , i.e. $D_{ii} = \sum_j A_{ij}$. The other entries are zeros.
3. Define $P = D^{-1}A$, the graph diffusion matrix.

□ Clean this up: get anisotropic equation, and clarify the role of the self affinity. When is it removed? When is laziness added?

P has several nice properties. The rows $P[i]$ give the transition probabilities of a single step random walk starting at point x_i ; each row $P[i]$ can be viewed as a probability distribution centered at x_i . This is preserved under powers of the matrix. The rows of P^t still sum to 1, and $P^t[i]$ now gives the probability distribution of a t -step random walk starting at x_i .

Although P is not symmetric, it is conjugate to a symmetric matrix, via $D^{0.5}PD^{-0.5} = D^{-0.5}AD^{-0.5}$, granting it a full basis of real-valued eigenvectors and eigenvalues. These eigenvectors are shared with the normalized graph Laplacian $L = I - D^{-0.5}AD^{-0.5}$. The eigenvalues of P lie between 0 and 1. Powering the matrix P^t thus corresponds to powering the eigenvalues λ_i^t of P , via diagonalization

$$P^t = \Psi \Lambda^t \Psi^T$$

This is similar to applying a low-pass filter to the graph. As t increases, the smallest eigenvalues decay fastest under repeated powering, and their corresponding eigenvector vanishes from the eigenbasis – leaving only the largest λ_i , whose eigenvectors trace global geometric features.

This is a remarkable feature of the diffusion matrix: the ability to “denoise” itself by iterating the random walk over larger time scales. Intuitively, the paths through the data most robustly trafficked by random walkers are those supported by multiple high-probability connections from independent starting points.

0.3 Related Work

0.3.1 Foreman Ricci Curvature

0.3.2 Hickock’s Curvature

0.3.3 Ollivier-Ricci Curvature

Developed by Yann Ollivier in 2007, *Coarse Ricci Curvature* (or sometimes, “Ollivier Ricci Curvature”) is a direct translation of Ricci curvature to discrete metric spaces like graphs ([ollivier2009RicciCurvatureMarkov?](#)). Several classical properties of Ricci curvature can be extended to the graph setting using Coarse Ricci Curvature. Ollivier has, for instance, proven versions of concentration inequalities, Bonnet Myers (more). Coarse Ricci Curvature

has, in this way, become something of a bridge between continuous and coarse geometry. The basis of this bridge is optimal transport, and specifically, the 1-Wasserstein distance.

In the Riemannian setting, Ricci curvature captures the phenomenon that, in positive curvature, “small spheres are closer (in transportation distance) than their centers are” (CITE 43 in ORC Paper). On the sphere, for instance, imagine two circles placed at the north and south poles: every point is closer to the corresponding point on the opposite pole than the centers. In negatively curved spaces, the discrepancy reverses, while in a flat space, the average distance between the points of the circles is the distance between the centers.

Coarse Ricci Curvature captures a similar phenomenon on graphs. Instead of spheres, it uses locally-centered probability distributions defined by random walks. And to measure the distance between these walks, it uses the 1-Wasserstein (or Earth Mover’s) distance. We’ll briefly define each.

The 1-Wasserstein distance is a measure of the distance between probability distributions. Given distributions μ_x and μ_y over some shared space X , the Wasserstein distance quantifies the smallest amount of “work” needed to transform one distribution into another, by transporting probability “mass” between pairs of points over the ground metric $d(x, y)$:

[!Info] Definition The 1-Wasserstein distance between distributions μ_x and μ_y is

$$W_1(\mu_x, \mu_y) := \inf_{\xi \in \Pi(\mu_x, \mu_y)} \int \int d(x, y) d\xi(x, y)$$

where the “transportation plan” ξ is drawn from the space $\Pi(\mu_x, \mu_y)$ of joint probability distributions over $X \times X$ which project onto μ_x and μ_y .

In the discrete setting, this translates naturally into an infimum over a summation.

$$W_1(\mu_x, \mu_y) := \inf_{\xi \in \Pi(\mu_x, \mu_y)} \sum_{x \in X} \sum_{y \in X} d(x, y) \xi(x, y)$$

What is the analog on a graph of a “small sphere” around a point? Ollivier replaces spheres with a family of measures $m_x(\cdot)$ defined for each point x , where 1. Each $m_x(\cdot)$ depends measurably on x , i.e. the map $x \rightarrow m_x$ is measurable. 2. Each $m_x(\cdot)$ has finite first moment, or *Jump*, i.e. for some $o \in X$ $\int d(o, y) m_x(y) dx < \infty$.

The *Jump* $J(\mu_x)$ of a measure, a measure of its concentration around a central point, is a concept to which we’ll return.

$$J(\mu_x) = \int_{y \in X} d(x, y) \mu_x(y) dx$$

In graphs, Ollivier defines these μ_x as the probability distributions created by a single-step random walk from the point x . With a transition probability α , and equal probability of

moving to each of x 's neighbors on the graph, $\mu_x(x) = (1 - \alpha)$ and $m_x(y) = \alpha$ if $y \in N(x)$ or 0 otherwise. This is analogous to defining $m_x = Pe_x$, if P is the diffusion matrix created from a binary adjacency matrix. Note, however, that there is nothing limiting us to binary adjacency matrices, or even single steps of diffusion; the two conditions above are equally satisfied by weighted adjacency matrices and t -step diffusions, and in sparse or noisy graphs, this may be desirable.

Definition

The *Coarse Ricci Curvature* between x and y is

$$\kappa(x, y) := 1 - \frac{W_1(m_x, m_y)}{d(x, y)}$$

There are a number of provisos attached to this definition, which tries to approximate a continuous phenomenon within discrete constraints. These constraints, and the relationship between Ricci and Ollivier's coarse Ricci curvature are illustrated Ollivier's Example 2.6 (**ollivier2009RicciCurvatureMarkov?**):

Let (X, d) be a smooth Riemannian manifold of dimension d and let vol be the Riemannian volume measure. Let $\epsilon > 0$ small enough and consider the ball of radius ϵ around each point x . Let $x, y \in X$ be two sufficiently close points. Let v be the unit tangent vector at x directed towards y . The coarse Ricci curvature along v is then

$$\kappa(x, y) = \frac{\epsilon^2 \text{Ric}(v, v)}{2(d + 2)} + o(\epsilon^3 + \epsilon^2 d(x, y))$$

Hence the coarse Ricci curvature applied to a manifold recovers the Ricci curvature, up to a scaling factor contingent on dimension, and plus an error term that grows with the radius of ball and distance between points.

Ollivier's choice not to scale $\kappa(x, y)$ by dimension is interesting, and likely motivated by his application of coarse Ricci curvature to graph-like spaces for which dimension isn't clearly defined, like social networks. Within our domain of point-cloud data, incorporating dimension may be desirable; without it, spaces of high dimension can be conflated with spaces of low negative curvature but high dimension.

A result on coarse Ricci curvature which will prove useful concerns the *contraction (or expansion) of measure* that occurs under diffusion in spaces of positive (or negative) curvature.

Proposition 20 (**ollivier2009RicciCurvatureMarkov?**)

Let (X, d, m) be a metric space with a random walk. Let $\kappa \in \mathbb{R}$. Then we have $\kappa(x, y) \geq \kappa$ for all $x, y \in X$ iff for any two probability distributions $\mu, \mu' \in \mathcal{P}(X)$ one has

$$W_1(\mu \star m, \mu' \star m) \leq (1 - \kappa)W_1(\mu, \mu')$$

Where

$$\mu \star m := \int_{x \in X} d\mu(x) m_x dx$$

0.4 Methods

0.4.1 Definition

Given samples $X \subseteq M$ and a flattening map $\Phi : X \rightarrow \mathbb{R}^d$,

The t -step *Diffusion Curvature* of x is

$$k_t(x) = 1 - \frac{W_1(\delta_x, p_X^t(x))}{W_1(\delta_x, p_{\Phi(X)}^t(x))}$$

{eq-definition}

Where p_X^t is the t -step random walk over X , and $p_{\Phi(X)}^t$ is the same over the flattened points $\Phi(X)$. In both cases, the W_1 distance is taken with respect to manifold distances.

0.4.2 Separating Geometry from Sampling: Neural Flattening

0.4.3 Connections to Ollivier-Ricci Curvature

Although diffusion curvature was designed for sampled manifolds, it extends naturally to the realm of more general graphs. Indeed, diffusion curvature can be seen as an node-wise adaptation of Ollivier Ricci curvature, the theoretically richest and highest performing edge-wise graph curvature [citations to Bastian’s paper on ORC expressivity]. Here we review the definitions of Ollivier-Ricci curvature and present theoretical connections between it and diffusion curvature. These motivate the use of diffusion curvature as substitute for Ollivier Ricci curvature on large, or noisy graphs where the latter method stumbles. [Present some of these in experiments]

Ollivier Ricci curvature is based in optimal transport, formalizing the classical intuition that in spaces of positive curvature, “spheres are closer than their centers” [cite ollivier]. In place of spheres, Ollivier uses diffused diracs; for distance, he uses the Wasserstein-1 distance with the shortest-path metric. Given points x, y in the metric space, with 1-step diffusions m_x and m_y , the Ollivier Ricci curvature of the edge between x and y is:

$$\kappa(x, y) := 1 - \frac{W_1(m_x, m_y)}{d(x, y)}$$

Local curvature always involves some comparison. Here, the comparison is between the manifold's optimal transport distance (the numerator), and the Euclidean optimal transport distance (which, helpfully, is just the distance in the denominator. You'll notice the similarity to diffusion curvature, which replaces the W_1 distance between two diffused distributions with the W_1 distance between a point and its t -step diffusion. We do this for both the manifold (in the numerator) and a Euclidean comparison space (in the denominator).

$$k_d(x, y) = 1 - \frac{W_1^M(\delta_x, m_x^t)}{W_1^E(\delta_x, m_x^t)}$$

The basis of diffusion curvature's comparison is the "spread" of diffusion as measured by $W_1(\delta_x, m_x^t)$. Intuitively, in regions of positive curvature, diffusion spreads less; neighborhoods with higher interconnectivity make random walks lazier. We can formalize this with reference to Ollivier Ricci curvature:

Proposition 1. Let (X, d, m) be a metric space equipped with a random walk, with coarse Ricci curvature bounded from below by some k such that $\kappa(x, y) \geq k$ for all $x, y \in X$. The Wasserstein Spread of Diffusion of a t step diffusion in X is bounded above by

$$W_1(\delta_x, m_x^t) \leq W_1(\delta_x, m_x) \frac{(1 - (1 - k)^t)}{k}$$

In particular, if $k > 0$ then $W_1(\delta_x, m_x^t) \leq \frac{W_1(\delta_x, m_x)}{k}$, and if $k = 0$, then $W_1(\delta_x, m_x^t) \leq tW_1(\delta_x, m_x)$.

Proof. First, we bound $W_1(m_x^t, m_x^{t+1})$ using Ollivier's Proposition 20 [citation needed] on concentration of measure. The proposition states that a lower bound on curvature, such as we have, implies that

$$W_1(\mu \star m, \mu' \star m) \leq (1 - k)W_1(\mu, \mu')$$

where here μ, μ' are two probability distributions and m is a random walk. This provides an easy lemma:

Lemma 1. Let (X, d, m) be a metric space with a random walk. Suppose there is some $k \in \mathbb{R}$ such that the coarse Ricci curvature $\kappa(x, y) \geq k$ for all $x, y \in X$. Then:

$$W_1(m_x^t, m_x^{t+1}) \leq (1 - k)^t W_1(\delta_x, m_x)$$

Proof. We proceed by induction. For $t = 0$, the above is true, as $W_1(m_x^0, m_x^1) = W_1(\delta_x, m_x^1) = W_1(\delta_x, m_x)$. Suppose it holds for $t - 1$, e.g.

$$W_1(m_x^{t-1}, m_x^t) \leq (1 - k)^{t-1} W_1(\delta_x, m_x)$$

Consider $W_1(m_x^{t-1} \star m, m_x^t \star m)$, the application of another step of diffusion. By Ollivier's Proposition 20, this distance is bounded above by

$$W_1(\mu_1 \star m, \mu_2 \star m) \leq (1-k)W_1(\mu_1, \mu_2)$$

So

$$W_1(m_x^{t-1} \star m, m_x^t \star m) \leq (1-k)W_1(m_x^{t-1}, m_x^t)$$

which, since the statement holds for $t-1$, yields

$$W_1(m_x^t, m_x^{t+1}) \leq (1-k)^t W_1(\delta_x, m_x)$$

To use this lemma, we can decompose our t -step diffusion into a sum of single step diffusions. By the triangle inequality,

$$W_1(\delta_x, m_x^t) \leq W_1(\delta_x, m_x) + W_1(m_x, m_x^2) + \dots + W_1(m_x^{t-1}, m_x^t)$$

By Lemma 1,

$$\leq W_1(\delta_x, m_x) (1 + (1-k) + (1-k)^2 + \dots + (1-k)^{t-1})$$

This truncated series is equal to $\frac{1-(1-k)^t}{1-(1-k)} = \frac{(1-(1-k)^t)}{k}$. If $k > 0$, then as $t \rightarrow \infty$, the infinite sum $\sum_{i=0}^t (1-k)^i$ converges to the geometric series $\frac{1}{1-(1-k)} = \frac{1}{k}$. Because the sum is monotonically increasing with t , the partial sum is upper bounded by the infinite sum. It follows that

$$W_1(\delta_x, m_x^t) \leq \frac{W_1(\delta_x, m_x)}{k}$$

If $k = 0$, then obviously $\sum_i^t (1-k)^i = t$.

The above asserts that the “spread” of diffusion is bounded from above by the Ollivier Ricci curvature of the region. To turn this measurement of spread into a signed curvature, we have only to introduce a comparison: the dimensional constant of the Euclidean spread of diffusion, $W_1^E(\delta_x, m_x^t)$. Using Proposition 1, we can directly bound k_D in terms of the Ollivier Ricci curvature:

$$1 - \frac{W_1^M(\delta_x, m_x) \frac{(1-(1-k)^t)}{k}}{W_1^E(\delta_x, m_x^t)} \leq k_D$$

A simple approximation of $W_1^E(\delta_x, m_x^t)$ is obtained by scaling the spread of a single-step diffusion by a factor of t , i.e. $tW_1^E(\delta_x, m_x)$. Using this, and noting that $W_1^E(\delta_x, m_x) \approx W_1^M(\delta_x, m_x)$,

$$1 - \frac{(1-(1-k)^t)}{tk} \leq k_D$$

Note: this analysis sidesteps the reality that tJ is a (possibly egregious) *overestimate* of the euclidean WSD. We can't actually just plug it in without pushing some indeterminate space inbetween the sides of the inequality

0.5 Results

Curvature is an easy quantity to find – indeed, at least two of the many recent curvature methods were defined *accidentally* [cite Steinerberger, myself]! The challenge is to make one’s definition robust to the bogeyman of real-world data, especially 1) noise and 2) high dimensions. Our benchmarks of existing methods, including Hickok & Blumberg’s, Ollivier Ricci Curvature, Adal-PCA [and Sritharan], [citations] reveal that all deteriorate quickly under noise, and most *fail entirely* in high-dimensional data. The dimension-independent, noise-resilient properties of the diffusion operator endow diffusion curvature with good performance on both of these axes.

But first, a sanity check. Does diffusion curvature recover the Gaussian curvature of basic 2-manifolds? Figure WAWA shows the diffusion curvature of a Torus, Saddle, and Ellipsoid, along with a scatter plot correlating diffusion curvature and Gaussian curvature. Figure WAWA2 places this in the context of existing methods.

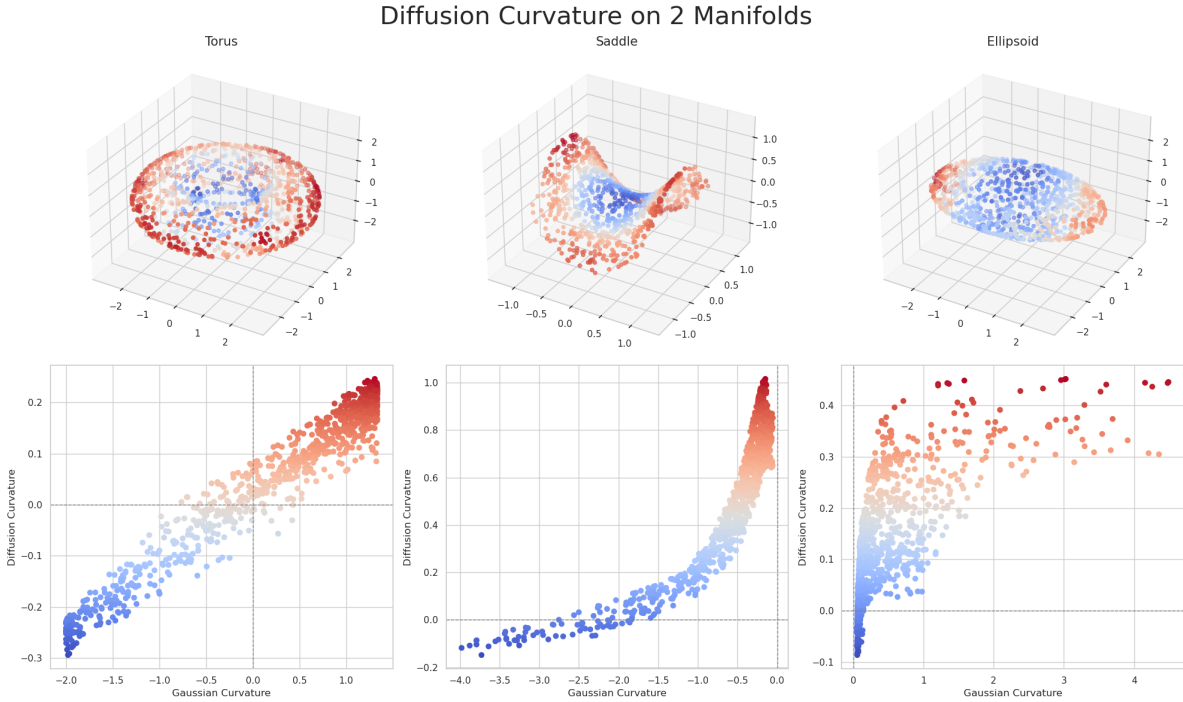


Figure 1: Diffusion Curvature vs Gaussian Curvature on 2-Manifolds.

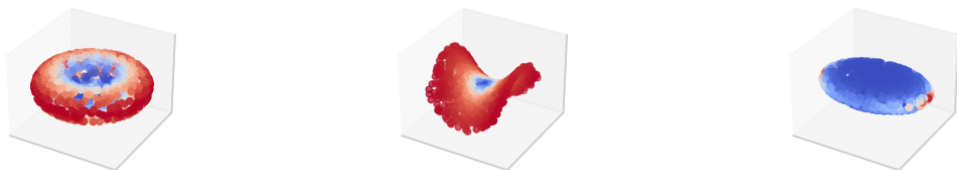
Source: [Standard libraries](#)

Though the correlation is strong – passing the ‘sniff test’ – this low-dimensional validation highlights two subtleties of our method. First, diffusion curvature, being an intrinsic, graph-based measurement, is susceptible to edge effects to a greater degree than extrinsic methods.

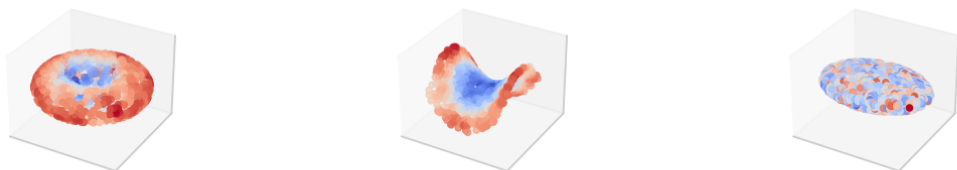
When diffusion hits the edges of the saddle, it rebounds, creating the false appearance of positive curvature.

Estimated Gaussian Curvatures of 2-Manifolds

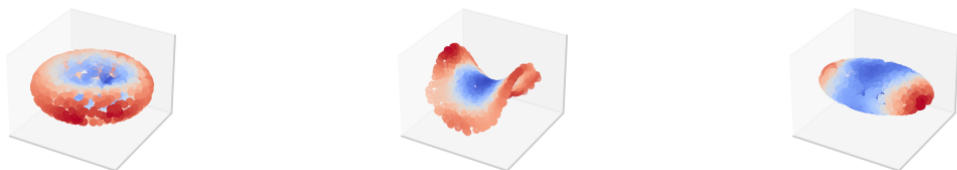
Ground Truth Curvature



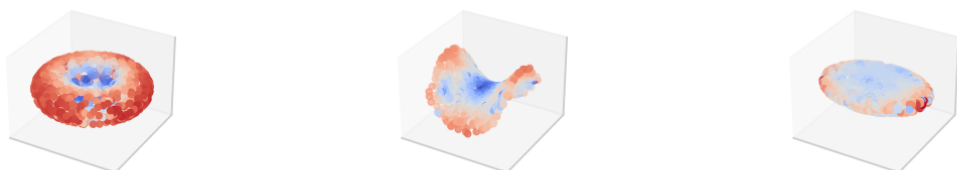
Diffusion Curvature



Unsigned Diffusion Curvature



AdaL-PCA



Hickok & Blumberg

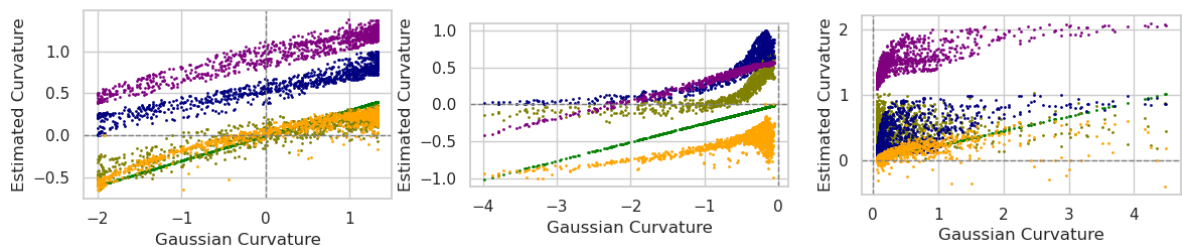
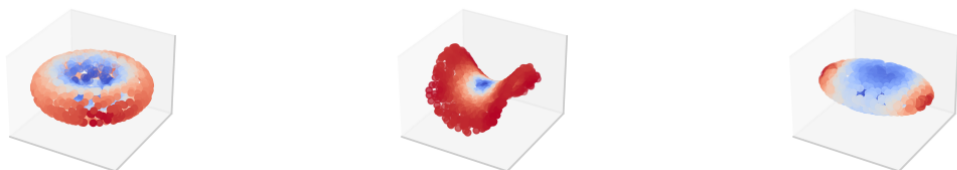


Figure 2: Diffusion Curvature vs Gaussian Curvature on 2-Manifolds.

Source: [Standard libraries](#)

The second subtly emerges in the context of related methods. Everything pictured does an excellent job of coloring the toy manifolds. But looking beyond this, *what matters?* Most methods don't care about the precise magnitude – or even exactly matching the correlations, as in the ellipsoid... %% mean vs gaussian curvature, and uniqueness of definitions%%

All of these methods in Fig WAWA2 perform well on well-sampled noiseless toy manifolds. In Table WAWA3, we see the results of adding Gaussian noise to each manifold.

![[CleanShot 2024-04-28 at 23.30.38_147B95A7.png]]

0.5.1 Differentiating Sign in High Dimensions

Most existing methods only quantify their performance in high dimensions on one or two test cases.

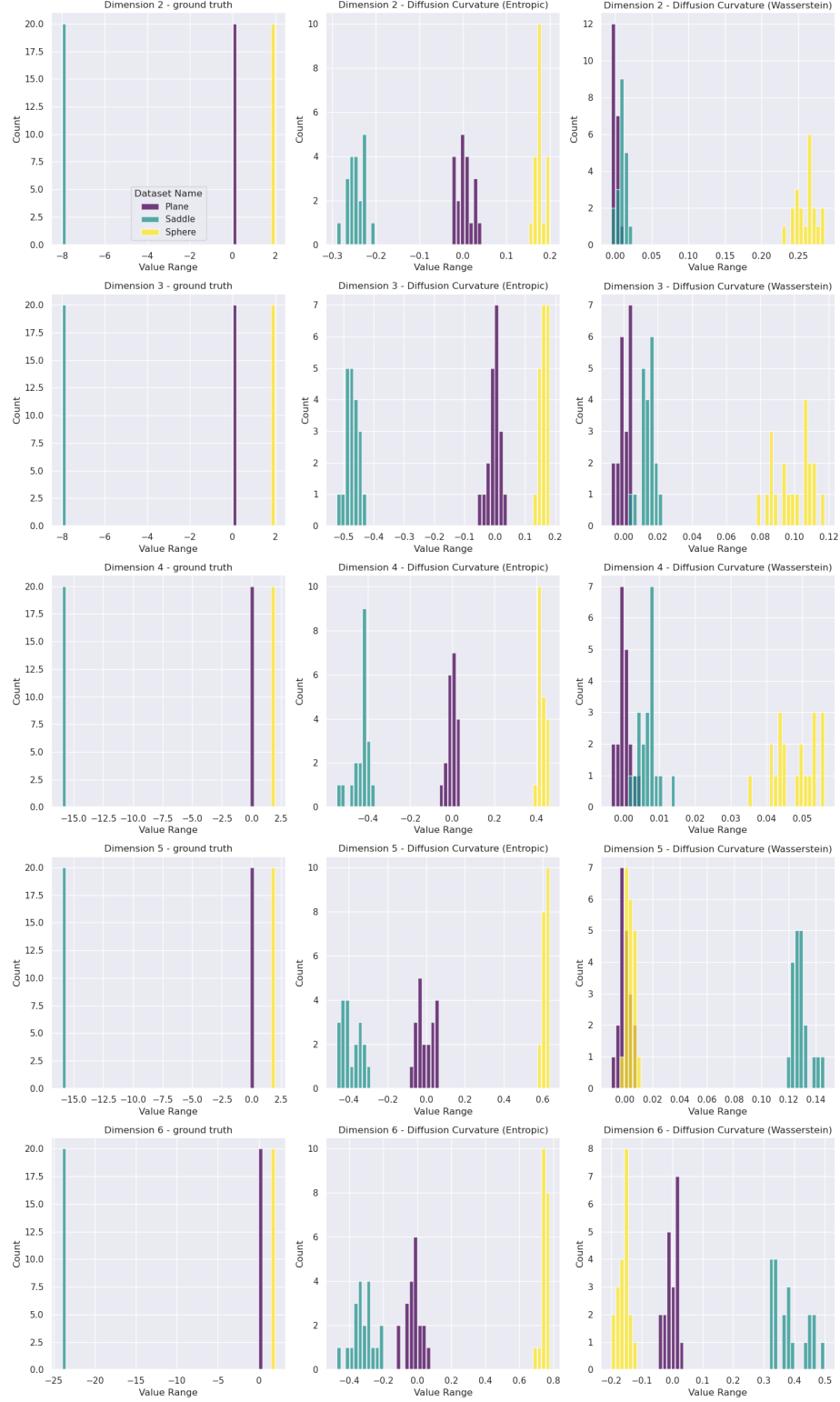


Figure 3: Predicted curvatures of Saddles and Spheres in dimensions 2-6. Diffusion Curvature robustly distinguishes between the signs of the data, even in high dimensions, and with relative sparsity.

Source: [Standard libraries](#)

0.5.2 Loss Landscapes

0.5.3 Curvature as a TDA Filtration

0.6 Conclusion

References

Bhaskar, Dhananjay, Kincaid MacDonald, Oluwadamilola Fasina, Dawson Thomas, Bastian Rieck, Ian Adelstein, and Smita Krishnaswamy. 2022. “Diffusion Curvature for Estimating Local Curvature in High Dimensional Data.” *Advances in Neural Information Processing Systems* 35: 21738–49. https://proceedings.neurips.cc/paper_files/paper/2022/hash/88438dc62fc5c8777e2b5f1b4f6d37a2-Abstract-Conference.html.